Chaos ARTICLE scitation.org/journal/cha

# Neuronal synchronization in long-range time-varying networks

Cite as: Chaos **31**, 073129 (2021); doi: 10.1063/5.0057276
Submitted: 19 May 2021 · Accepted: 21 June 2021 ·
Published Online: 14 July 2021



Sarbendu Rakshit,[1] Soumen Majhi,[1,2] Jürgen Kurths,[3,4] and Dibakar Ghosh[1,a)]

## AFFILIATIONS

[1]Physics and Applied Mathematics Unit, Indian Statistical Institute, 203 B. T. Road, Kolkata 700108, India
[2]Department of Mathematics, Bar-Ilan University, Ramat-Gan 5290002, Israel
[3]Potsdam Institute for Climate Impact Research - Telegraphenberg A 31, Potsdam 14473, Germany
[4]Department of Physics, Humboldt University Berlin, Berlin 12489, Germany

**Note:** This paper is part of the Focus Issue, In Memory of Vadim S. Anishchenko: Statistical Physics and Nonlinear Dynamics of Complex Systems.

[a)]**Author to whom correspondence should be addressed:** dibakar@isical.ac.in

## ABSTRACT

We study synchronization in neuronal ensembles subject to long-range electrical gap junctions which are time-varying. As a representative example, we consider Hindmarsh–Rose neurons interacting based upon temporal long-range connections through electrical couplings. In particular, we adopt the connections associated with the direct 1-path network to form a small-world network and follow-up with the corresponding long-range network. Further, the underlying direct small-world network is allowed to temporally change; hence, all long-range connections are also temporal, which makes the model much more realistic from the neurological perspective. This time-varying long-range network is formed by rewiring each link of the underlying 1-path network stochastically with a characteristic rewiring probability $p_r$, and accordingly all indirect $k$ ($> 1$)-path networks become temporal. The critical interaction strength to reach complete neuronal synchrony is much lower when we take up rapidly switching long-range interactions. We employ the master stability function formalism in order to characterize the local stability of the state of synchronization. The analytically derived stability condition for the complete synchrony state agrees well with the numerical results. Our work strengthens the understanding of time-varying long-range interactions in neuronal ensembles.



**The process of synchronization is a subject of distinguished importance in neuronal systems. From neuronal communication and plasticity to cognitive processes, synchronous spatiotemporal patterns[1,2] play crucial roles. Significant attention has been paid to this phenomenon of neuronal synchronization,[3,4] while considering diverse aspects of synchrony and also a number of complexities in the topology of the underlying network. In this context, time-varying networks are now one of the best ways to describe a number of natural scenarios including neuronal synaptic communications. Moreover, in recent times it has been demonstrated that, in certain networked systems, entities interact not only through the direct short-range connections; rather, they can communicate via distant long-range paths as well. But, so far, not only in the study of neuronal processes but from many other perspectives, mostly time-varying networks have been considered along with only direct interactions among the constituents, and the effects of long-range connections are yet to be explored under the temporal connectivity framework. In this article, we attempt to fill this gap and predominantly consider both aspects of network science and present our results on neuronal synchrony in long-range networks with time-varying synaptic interactions. We specifically assume electrical gap junctions as the medium of communication among the neurons and small-world network model as the underlying network platform for our work, while casting the dynamics of neurons by that of the Hindmarsh–Rose systems. As principal results, we find that by considering the time-varying long-range interactions the neuronal synchronization enhances significantly, and we have been able to demonstrate this claim both analytically and through rigorous numerical results. Specifically, we analyze the stability of this neuronal synchronization state by the celebrated master stability function approach.**

## I. INTRODUCTION

Interaction among natural systems takes place in several ways, which influences the underlying dynamics significantly. In fact, for these coupled systems, various interwoven connectivity patterns are responsible for their proper functioning. The theory of complex networks[5,6] has emerged to be the unifying paradigm explaining scenarios behind such systems and processes across disciplines ranging from physics and mathematics to biology and engineering. During the last few decades, the process of synchronization[7–10] in complex networks, specifically in temporal networks,[11] has been explored with various network topologies and coupling configurations.[12–24] In the earlier works, mostly the temporal network topologies were assumed to be composed of direct interactions among the nodes, although in many real situations the type of interactions is short-range as well as long-range. The coaction between the network structure and dynamics in such time-varying long-range interactions can result in emerging collective behavior, which are relevant in several physical, biological, and social scenarios.

Several natural systems interact through long-range interactions;[25,26] specifically, this type of interaction has been found to be present in a number of physical[27] and biological[28] scenarios. Particularly, this type of interaction architecture has a significant effect on the one-dimensional Ising spin model with power-law long-range interaction[29] and spin-glass models.[30] However, such phase transitions are not possible for lower values of the power-law exponent. Long-range interaction controls the connectivity with certain scaling among the animal brain neurons.[31] The power-law type long-range interactions have also been observed in plasmas[32] and even in spatial ecology of species dispersal within different patches.[33] Moreover, long-distant movements of butterfly *Euphydryas aurinia* ensues an inverse power law.[34]

The scaling parameters associated with long-range interactions in a network of oscillators efficiently control the interaction range and strength.[35] In the context of synchronization, the influence of long-range coupling has been previously studied in phase oscillators,[36] coupled map lattice,[35] and biological networks.[37] Phase transition from a synchronized to asynchronous state can be witnessed in a one-dimensional ring of mismatched phase oscillators whenever the range of interactions is decreased.[38] Few studies so far have focused on long-range interactions from the perspective of analyzing synchronization in networked dynamical systems. For instance, authors in Refs. 39 and 40 investigated synchronizability over lattices for ensembles of phase oscillators, and also in the case of maps.[41] Synchronization of coupled oscillators owing to long-range interaction with different forms of decaying couplings was studied in Ref. 42. On the other hand, the emergence of oscillation death in a repulsively coupled Stuart–Landau system as a result of long-range interactions,[43] and the persistence of metapopulation in the presence of long-range species dispersal[44] have been studied very recently.

This way, most of the previous studies have assumed static long-range interactions in which the underlying 1-path network topology remains unchanged for all the course of time duration. However, several real-world networks are not time-static, rather the links appear, disappear, or get rewired at different timescales.[45] These temporal characteristics are encountered in the context of social interactions,[46] where the relationship among the individual social units varies temporally. Temporal evolution is an inherent feature of various natural and man-made networks, and only at large timescales a static approximation is valid.[47] In several real-world situations, such as consensus problem,[48] disease spreading,[49] functional brain networks,[50] person-to-person communication,[51] power transmission system,[52] chemotaxis,[53] and wireless sensor networks,[54] temporal interactions have wide applicability. Also, time-varying connectivities exist in several biological scenarios such as protein–protein interaction, metabolism, gene-regulatory networks,[55] etc.

In neuronal networks, neurons communicate via electrical gap junction to carry out a number of biological functions.[56–58] But, neuronal communications may not be present all the time, prevailing links may disappear and new connections may form over time. This causes the formalism of temporal networks to be highly effective for modeling neuronal communication, as the electrical communication among the neurons can be imitated by a time-varying connection.[11] Few earlier studies have demonstrated this time-varying nature of neuronal interactions.[50,59,60] Thus, for further understanding of networked neuronal dynamics,[61–64] a shift from static to evolving neuronal communication is essential. Bassett and Bullmore[65] investigated the small-world property in the structure of the functional brain network. Recently, the small-world pattern of the brain network has also been studied in Ref. 66. On the other hand, neuronal networks manifest long-range connectivity from a number of perspectives, determining the functional-anatomical organization of the cortex and hence plays crucial roles in large-scale brain-wide interactions.[67–70]

In this article, we assume a neuronal ensemble in which the dynamics of each neuron is modeled by Hindmarsh–Rose systems, and the communication among the neurons occurs via electrical gap junctions. Since this type of interaction is bidirectional in nature, we will consider bidirectional electrical synapses through which the neuronal systems communicate on top of small-world networks. Since the interaction among neurons is essentially time-varying in nature, we contemplate with time-evolving connections having a certain rewiring probability. With this setup of a temporal long-range neuronal network, we concentrate on complete neuronal synchrony and its stability. Further, as we consider temporal long-range networks, we analyze the role of the network rewiring probability on complete neuronal synchronization. Here, our primary goal is to elucidate this emerging phenomenon in networks exhibiting temporal long-range connections via an illustration inspired by characteristics of neuronal oscillators communicating through electrical gap junctions. Here, we analyze the linear stability using the master stability function (MSF) approach that quantifies the local stability of synchronization manifold under infinitesimal perturbations. We derive the necessary and sufficient condition for such local stability.

## II. THE NETWORK MODEL

Consider a network consisting of $N$ nodes, where a $l$-dimensional dynamical system is associated with each node. The dynamical state of the $i$th node is represented by a vector $\mathbf{x}_i$ and its evolution function $F(\mathbf{x}_i)$, which is continuous and differentiable. We consider the diffusive coupling function $\Gamma(\mathbf{x}_j - \mathbf{x}_i)$ between the nodes $i$ and $j$, where $\Gamma$ stands for the inner-coupling matrix. The

entire coupled system obeys the following evolution equation:

$$\dot{\mathbf{x}}_i = F(\mathbf{x}_i) + \sum_{k=1}^{k_{\max}(t)} \epsilon_k \sum_{j=1}^{N} \mathscr{A}_{ij}^{[k]}(t)\Gamma(\mathbf{x}_j - \mathbf{x}_i), \tag{1}$$

where $i = 1, 2, \ldots, N$. At time $t$, the adjacency matrix corresponding to the $k$-path network is represented by $\mathscr{A}^{[k]}(t)$. The element $\mathscr{A}_{ij}^{[k]}(t) = 1$ if the $i$th and $j$th nodes are $k$-path connected and 0 otherwise. At each time instant $t$, the entire network is rewired with probability $p_r$. In other words, with probability $p_r$ the network gets replaced by a new network at each time and hence the adjacency matrix $\mathscr{A}^{[k]}(t)$ for each $k$-path network becomes a function of time. Small $p_r$ implies that the network is almost static. However, a large value of $p_r$ signifies that the networks are changing rapidly. Here, $F : \mathbb{R}^l \to \mathbb{R}^l$ is a function describing the isolated node dynamics and $\epsilon_k$ is the interaction strength for $k$-path network between $i$th and $j$th nodes where the distance between them $d(i, j) = k$. So, the $i$th and $j$th nodes are $k$-path connected, where $1 \le k \le k_{max}(t)$ with $k_{max}(t)$ being the diameter of the network at the time instance $t$. $\Gamma$ determines the state variable through which the nodes are coupled to each other. The entries of the time-varying $k$-path adjacency matrix $\mathscr{A}^{[k]}(t)$ [for $1 \le k \le k_{max}(t)$] are as follows:

$$\mathscr{A}_{ij}^{[k]}(t) = \begin{cases} 1 & \text{if } d(i,j) = k \text{ at the time instant } t, \\ 0 & \text{otherwise.} \end{cases}$$

Then, the time-varying $k$-path Laplacian matrix $\mathscr{L}^{[k]}(t)$ can be described as

$$\mathscr{L}_{ij}^{[k]}(t) = \begin{cases} -\mathscr{A}_{ij}^{[k]}(t), & \text{if } i \neq j, \\ \sum_{j=1}^{N} \mathscr{A}_{ij}^{[k]}(t), & \text{if } i = j. \end{cases}$$

Since the considered interactions are essentially bidirectional, therefore $\mathscr{A}^{[k]}(t)$ and hence $\mathscr{L}^{[k]}(t)$ are both symmetric matrices of order $N$ for each $k$ and time instant $t$. This implies $\mathscr{L}^{[k]}(t)$ $(k = 1, 2, \ldots, k_{max})$ is orthogonally diagonalizable through its basis of eigenvectors.

Here, we examine the effect of a power-law decay of the coupling strength $\epsilon_k$ between the nodes with the shortest distance $k$ $(1 \le k \le k_{max})$. In particular, we choose $\epsilon_k = \frac{\epsilon}{k^\alpha}$, where $\alpha$ is the exponent of the power law that explains the decay rate. The underlying network has been considered to be of small-world architecture. Specifically, we choose the Watts–Strogatz (WS) graph model[71] starting with non-local ring of $N$ number of nodes, $k_{sw}$-nearest neighbor on each side and $p_{sw}$ as the edge-rewiring probability.

This model is inspired by the questions discussed in Sec. I that the neuronal networks possess time-varying connections. Next, we explore the influence of long-range interactions determined by the electrical gap junctional coupling with power-law scaling on top of a small-world network of coupled Hindmarsh–Rose oscillators. By changing the network's parameters, we demonstrate that the temporal long-range interaction may generate neuronal synchronization in such coupled systems. To the best of our knowledge, such temporal long-range interactions in neuronal oscillators have not been investigated before in the context of synchronization. We further provide a MSF based linear stability analysis to establish the stability of the complete synchronization state.

## III. BIOLOGICAL NETWORK OF NEURONS

Neuronal networks are one of the most realistic examples of temporal long-range interactions, since the electrical synapses are known to evolve with time. This elementary functional connection enables information to be transferred efficiently among the neurons. Gap junctions directly connect the cytoplasm of adjacent cells in the case of electrical synapses. Between the pre-synaptic and the post-synaptic neurons, a direct bidirectional passage of electric current, cyclic AMP, calcium, and inositol-1,4,5 trisphosphate occurs. For such synaptic interactions, the distance between the membranes of pre-synaptic and post-synaptic neurons is approximately 3.5 nm,[72] i.e., therefore, they are extremely close to each other. Generally, in the mammalian brain, electrical gap junctions are broadly distributed, which can detect the coincidence of concurrent subthreshold depolarizations for a network of interacting neurons, thus increasing neuronal excitability and neuronal synchronization. Electrically coupled neuronal networks are observed during brain development post-injury,[73] and it is postulated to encode neural synchronization, a denomination that emphasizes the character of their bi-directional substance.[74] Apart from the electrical transmission, inter-neuronal communications may take place through chemical and ephaptic couplings, in which information among the neurons is rapidly transferred chemically via neurotransmitter molecules and generation of electric fields, respectively. In particular, the coaction of the electrical and chemical synaptic interactions on the synchronization and rate of information flow in neuronal networks has also been studied in Ref. 75.

Considering $N$ Hindmarsh–Rose (HR) model neurons connected by long-range electrical synapses, the dynamics of such neuronal network can be described by

$$\begin{aligned} \dot{x}_i &= y_i - a x_i^3 + b x_i^2 - z_i + I + \epsilon \sum_{k=1}^{k_{\max}(t)} \frac{1}{k^\alpha} \sum_{j=1}^{N} \mathscr{A}_{ij}^{[k]}(t)(x_j - x_i), \\ \dot{y}_i &= c - d x_i^2 - y_i, \\ \dot{z}_i &= r(s(x_i - x_0) - z_i), \quad i = 1, 2, \ldots, N. \end{aligned} \tag{2}$$

Here, $x_i$ is the membrane potential of the $i^{th}$ neuron, $y_i$ is associated with the fast $Na^+$ or $K^+$ current, and $z_i$ with the slow $Ca^{2+}$ current, in which $r$ is the modulator of the slow dynamics. Also, $\epsilon$ quantifies the electrical coupling strength. Throughout this contribution, the system parameters are considered as $a = 1, b = 3, c = 1$, $d = 5, I = 3.25, r = 0.005, s = 4$, and $x_0 = -1.6$, for which the membrane potential of the isolated HR oscillators shows a multi-time scale bursting behavior in a chaotic regime.

We would now like to mention here that functional brain networks derived from electroencephalogram (EEG) and functional magnetic resonance imaging (fMRI) experiments show characteristics of small-world networks[76–79] discriminated by short average path length and high local clustering. So, in our long-range network structure imitating neuronal networks, the communication through electrical gap junctions is modeled to possess a small-world topology with the average degree $2k_{sw}$, formed by the Watts–Strogatz (WS) network algorithm.[71] $\mathscr{L}^{(1)}$ denotes the zero row sum 1-path Laplacian matrix. To construct such network, we start with $N$ nodes, initially with a non-local ring network architecture where each node is adjacent with $k_{sw}$ nearest neighbors on both the sides. Then,

we reconnect (avoiding dual links) these initial links to randomly chosen distant nodes with the probability $p_{sw}$.

## IV. COMPLETE NEURONAL SYNCHRONIZATION: NUMERICAL ILLUSTRATION

In this section, we present our numerically obtained results. The time-varying long-range dynamical network given in Eq. (2) is numerically integrated using the fourth order Runge–Kutta method over $3 \times 10^5$ time iterations, using 0.01 as the integration time step. In particular, we assume a network comprised of $N = 200$ HR neurons. The initial condition for each oscillator is randomly chosen from the phase space of the chaotic attractor. Next, we define the complete synchronization error in the network as follows:

$$E = \left\langle \frac{1}{N-1} \sum_{j=2}^{N} \sqrt{(x_j - x_1)^2 + (y_j - y_1)^2 + (z_j - z_1)^2} \right\rangle_t , \quad (3)$$

where the time average $\langle \cdot \rangle_t$ is calculated over a sufficiently large time duration (chosen as $10^5$ time steps here). Therefore, for the state of complete neuronal synchrony, $E$ becomes zero necessarily and yields non-zero values for the state of desynchrony.

Here, our primary focus is to perceive the effect of the network architecture on the neuronal synchrony in the time-varying long-range network. We choose the system parameters of the individual HR neurons in a chaotic bursting regime and concentrate on the sub-set of network parameters and coupling strength. So, we investigate the spatiotemporal dynamics subject to the variation of the parameters $p_{sw}$, $p_r$, and $\epsilon$.

We start by looking at the evolution of $E$ [as in Eq. (3)] for varying network and coupling parameters with the intention of understanding the emergence of neuronal synchronization in system (2). For this, we choose the small-world probability $p_{sw} = 0.1$ with $k_1 = 3$. Figure 1(a) depicts the variation in $E$ in terms of the rewiring probability $p_r$ for several values of $\alpha$, with fixed $\epsilon = 0.5$. As can be seen there, it is discernible that the increasing $p_r$ effectively promotes neuronal synchronization irrespective of the chosen values of $\alpha$. Nonetheless, $\alpha$ also has a significant influence on the emergence of synchrony. To be precise, as higher the value of $\alpha$, as higher the $p_r$ required in order to achieve complete synchronization. We have chosen five exemplary values of $\alpha$ and the corresponding error curves demonstrate this fact. Similarly, next we plot $E$ with respect to $p_r$ for several values of the interaction strength $\epsilon$, while keeping $\alpha$ fixed at $\alpha = 2.5$ [cf. Fig. 1(b)]. Here again, we see that an increasing $p_r$ favors synchrony. This is because the network switches then more rapidly, and neuronal cells get the opportunity of interacting with the cells otherwise non-interacting. However, in contrast to the previous observation on the effects of $\alpha$, here increasing values of $\epsilon$ enhance the appearance of neuronal synchrony. Since $\epsilon$ accounts for the coupling strength among the neurons, higher values of it make the synchronization easier. *Thus, our observation clarifies that the coupling strength $\epsilon$ and the long-range exponent $\alpha$ show conflicting effects on the appearance of synchrony, the first one enhances, while the second one undermines neuronal synchronization. Also, fast network switching significantly amplifies the level of synchrony.*

We therefore focus on the interplay between the two coupling parameters, namely, the long-range exponent $\alpha$ and the interaction strength $\epsilon$. In order to study their combined impact in detail, we plot the synchronization region in the $(\epsilon, \alpha)$ plane in Fig. 2, where the color bar denotes the variation of $E$. Figure 2(a) shows how synchrony appears for simultaneous variations in $\epsilon \in [0, 1]$ and $\alpha \in [0, 5]$ whenever $p_r = 10^{-6}$. As observed, increasing $\epsilon$ induces

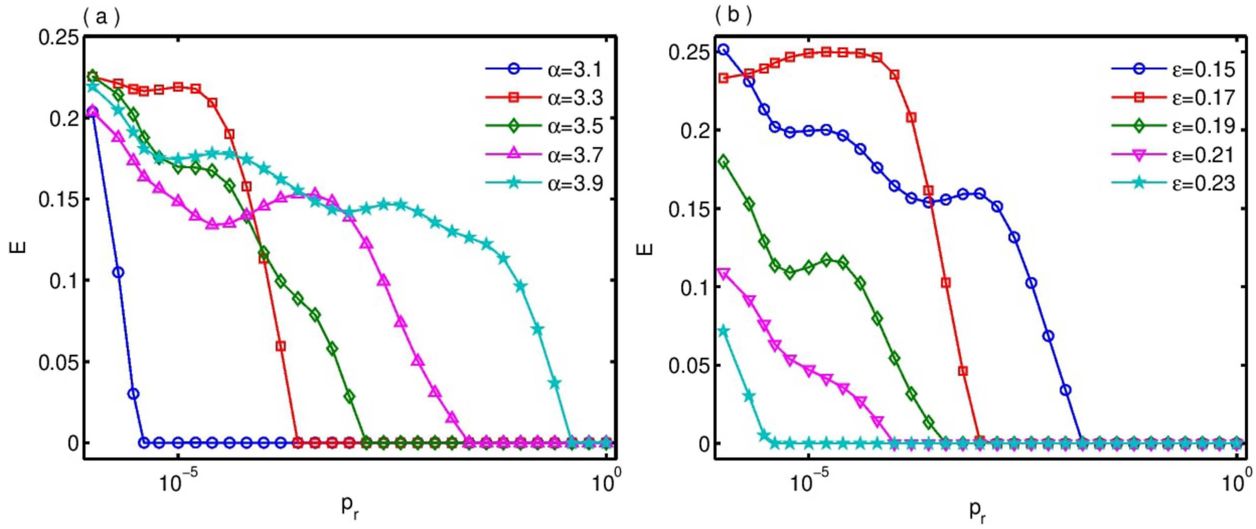


**FIG. 1.** Variation of $E$ in terms of the rewiring probability $p_r$ for different combinations of $\epsilon$ and $\alpha$. (a) $\alpha = 3.1$ (blue circle curve), $\alpha = 3.3$ (red square curve), $\alpha = 3.5$ (green diamond curve), $\alpha = 3.7$ (magenta triangle curve), and $\alpha = 3.9$ (cyan star curve). For this sub-figure, the other parameters' values are fixed at $\epsilon = 0.5$, $k_{sw} = 3$, and $p_{sw} = 0.1$. (b) $\epsilon = 0.15$ (blue circle curve), $\epsilon = 0.17$ (red square curve), $\epsilon = 0.19$ (green diamond curve), $\epsilon = 0.21$ (magenta triangle curve), and $\epsilon = 0.23$ (cyan star curve). For this sub-figure, the other parameters' values are fixed at $\alpha = 2.5$, $k_{sw} = 3$, and $p_{sw} = 0.1$.

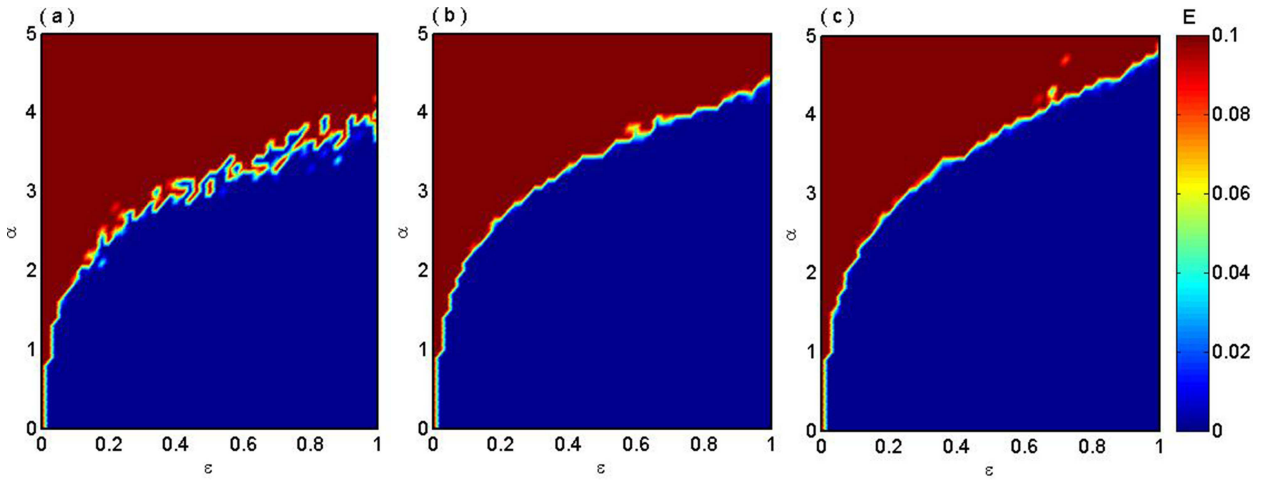


**FIG. 2.** Parameter space in the $(\epsilon, \alpha)$ plane in terms of $E$ for the time-varying long-range neuronal network with (a) $p_r = 10^{-6}$, (b) $p_r = 10^{-4}$, and (c) $p_r = 10^{-2}$. The network parameter values are fixed at $k_{sw} = 3$ and $p_{sw} = 10^{-1}$.

synchrony, whereas increasing $\alpha$ hinders it so that as $\alpha$ grows, higher $\epsilon$ is required to attain complete synchrony. Here, we mention that for the network rewiring probability being very small, the whole network acts like a static network (though not necessarily completely static). So, next we choose a higher switching probability $p_r = 10^{-4}$ and plot a similar phase diagram in Fig. 2(b). In this case, the network switching becomes more frequent and hence synchrony originates for smaller values of the coupling parameters. For even higher $p_r = 10^{-2}$, this enhancement becomes much stronger as the network switches much faster [cf. Fig. 2(c)]. The synergy between $\epsilon$ and $\alpha$ from the perspective of neuronal synchrony remains the same for any value of $p_r$.

So far, the results we have discussed contemplates with fixed small-world probability $p_{sw}$. But, $p_{sw}$ is one of the most important parameters in our study as it determines the randomness present in the network at any instant of time. To elucidate this, we depict the variation in the error $E$ in the $(\epsilon, p_{sw})$ parameter space in Fig. 3 for a variety of values of $\alpha$, where we have fixed $p_r = 10^{-3}$. Figure 3(a) shows the phase diagram for $\alpha = 5.0$ from which it is easily understandable that for increasing $p_{sw}$ lower values of $\epsilon$ turn out to be sufficient for synchronization, as $p_{sw}$ induces randomness in the interactions and connects even long-distant neurons in the network. This phenomenon remains unaltered for any lower $\alpha = 4.0,\ 3.0,\ 2.0$, and also $\alpha = 1.0$, with the difference that for lower $\alpha$ the network approaches the global connectivity limit and hence synchrony becomes easier to arise. Finally, whenever $\alpha = 0$, the networked system becomes globally coupled and therefore synchrony emerges right after $\epsilon$ exceeds a very small value.

Finally, we examine the role of the power-law exponent $\alpha$ with the small-world network probability $p_{sw}$ on the onset of complete synchrony. The desynchrony and synchrony regions are plotted in the $(\alpha, p_{sw})$ plane in Fig. 4, while considering four different values of the coupling strengths: (a) $\epsilon = 0.1$, (b) $\epsilon = 0.2$, (c) $\epsilon = 0.6$, and (d) $\epsilon = 1.0$. The probability of the network rewiring is fixed at $p_r = 10^{-3}$ with $k_{sw} = 3$ (i.e., with the average degree $2k_{sw} = 6$ of the SW network). For all the four values of $\epsilon$, there is an enhancement of the synchronization with respect to $p_{sw}$, however monotonic deenhancement in terms of $\alpha$. Interestingly, here we find that for a sufficiently high coupling strength and $p_{sw}$, synchronization can be achieved even for high values of $\alpha$.

## V. ANALYTICAL THEORY

In this section, we analytically derive conditions for the local stability of synchronization by using the fast switching stability criterion[80] and the MSF approach.[81] The fast switching stability criterion suggests that if the network of oscillators synchronizes for the static time average of the topology, then the network will synchronize with the time-varying topology if the time average is achieved for sufficiently fast switching. Fast rewiring of the underlying network overcomes the incoherent motion of the coupled systems suggested by the stagnant underlying network. This criterion yields a sufficient condition for stable synchronization solution for a rapidly switching underlying network consisting only of short-range interactions. For the main result, the authors proved that if there exists a constant $T$ such that for all $t \in \mathbb{R}$, $\bar{B} = \frac{1}{T}\int_t^{t+T} B(\tau)\, d\tau$, and the system $\dot{\mathbf{y}}(t) = [A(t) + \bar{B}]\mathbf{y}(t)$ is asymptotically stable. Then, the associated time-varying system $\dot{\mathbf{x}}(t) = [A(t) + B(t)]\mathbf{x}(t)$ will also exhibit asymptotically stable solution for sufficiently fast-switching.

Let, $\bar{\mathscr{A}}^{[k]}$ be the time-averaged $k$-path adjacency matrix of the electrical synaptic network, and $\bar{\mathscr{L}}^{[k]}$ be the corresponding Laplacian matrix. Assume that $\left\{0, \bar{\gamma}_2^{[k]}, \bar{\gamma}_3^{[k]}, \ldots, \bar{\gamma}_N^{[k]}\right\}$ denotes the set of eigenvalues of the time-averaged $k$-path Laplacian $\bar{\mathscr{L}}^{[k]}$. There exists a sufficiently large constant $T$ such that $\bar{\mathscr{L}}^{[k]} = \frac{1}{T}\int_t^{t+T} \mathscr{L}^{[k]}(\tau)\, d\tau$.

We devote now to the local stability analysis of neuronal synchronization. Here, we consider for sufficiently fast rewiring[80] that each time-varying $k$-path network can be well approximated

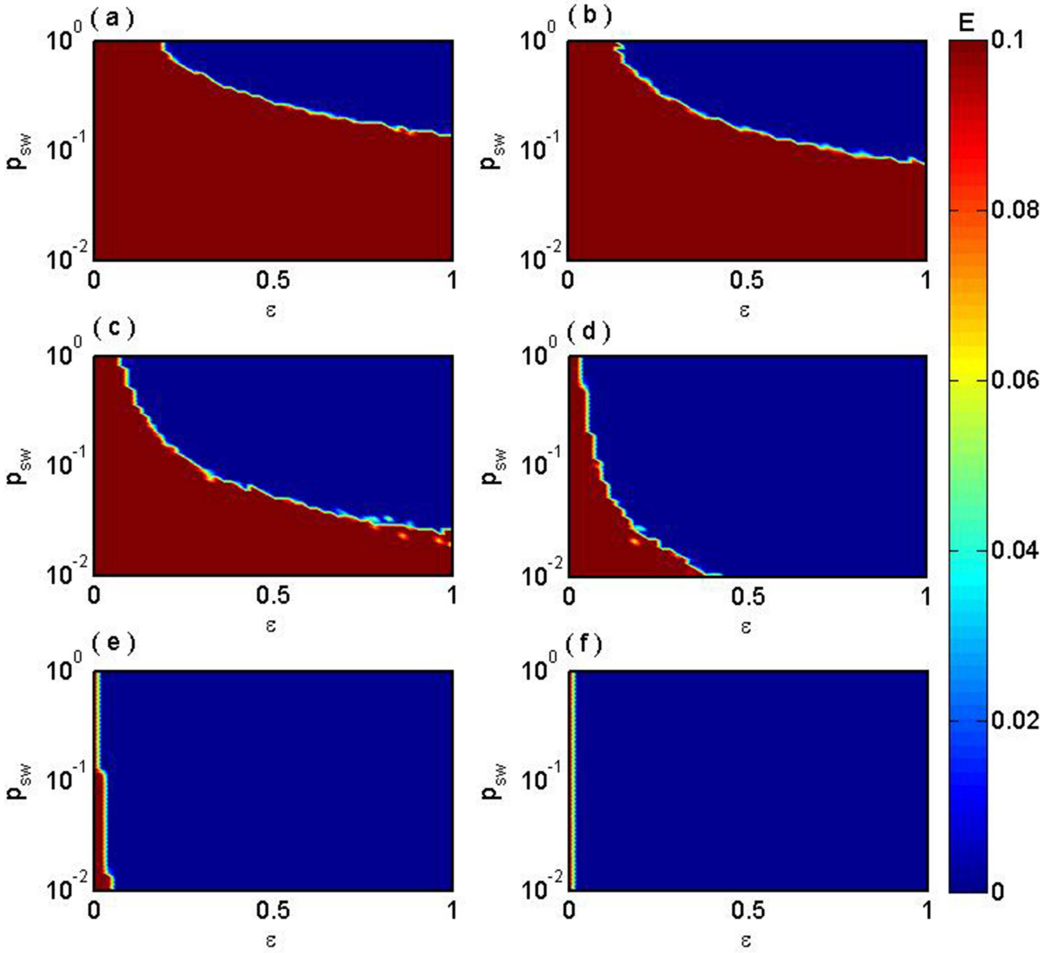


**FIG. 3.** Variation of $E$ in the $(\epsilon, p_{sw})$ phase plane for (a) $\alpha = 5.0$, (b) $\alpha = 4.0$, (c) $\alpha = 3.0$, (d) $\alpha = 2.0$, (e) $\alpha = 1.0$, and (f) $\alpha = 0.0$. Other parameter values are fixed at $k_{sw} = 3$ and $p_r = 10^{-3}$.

by the corresponding time-averaged static network. For complete synchrony, the individual dynamical units yield an identical trajectory at an appropriate coupling strength. Then, we assume that the entire network evolves synchronously with $\mathbf{x}_i(t) = \mathbf{x}_0(t)$ for all $i = 1, 2, \ldots, N$. $\mathbf{x}_0(t)$ is the state variable for the manifold of complete synchrony, whose dynamics can be written as $\dot{\mathbf{x}}_0 = F(\mathbf{x}_0)$. From the synchronization trajectory $\mathbf{x}_0(t)$, if we perturb the $i$th node with an amount $\delta\mathbf{x}_i(t)$, then we can write $\mathbf{x}(t) = \mathbf{x}_0(t) + \delta\mathbf{x}_i(t)$. If we consider the perturbation of all the systems in vectorial from, then we have $\delta\mathbf{x}(t) = [\delta\mathbf{x}_1(t)^{tr}, \delta\mathbf{x}_2(t)^{tr}, \ldots, \delta\mathbf{x}_N(t)^{tr}]^{tr}$. Here, $\mathbf{z}^{tr}$ denotes the transpose of the vector $\mathbf{z}$. Now linearizing around the trajectory $\mathbf{x}_0(t)$, the variational equation of the error system yields

$$\delta\dot{\mathbf{x}}(t) = [I_N \otimes JF(\mathbf{x}_0) - \sum_{k=1}^{k_{max}} \epsilon_k \mathscr{L}^{[k]}(t) \otimes \Gamma]\delta\mathbf{x}. \tag{4}$$

Considering that the temporal network exhibits a time-static averaged network for sufficient fast rewiring, then there exists a constant $T$ satisfying

$$\frac{1}{T}\int_t^{t+T} \mathscr{L}^{[1]}(\tau)\, d\tau = \bar{\mathscr{L}}^{[1]}. \tag{5}$$

Assuming $\bar{\mathscr{L}}^{[k]} = \frac{1}{T}\int_t^{t+T} \mathscr{L}^{[k]}(\tau)\, d\tau$ for all $2 \le k \le K_{max}$.

The corresponding time-averaged system can be written as

$$\dot{\mathbf{y}}_i = F(\mathbf{y}_i) + \sum_{k=1}^{K_{max}} \epsilon_k \sum_{j=1}^{N} \bar{\mathscr{A}}_{ij}^{[k]} \Gamma(\mathbf{y}_j - \mathbf{y}_i). \tag{6}$$

When complete synchronization occurs in this averaged networked system, the evolution equation of this solution is also $\dot{\mathbf{y}}_0 = F(\mathbf{y}_0)$, which is the same as for the time-varying networks. So, we may

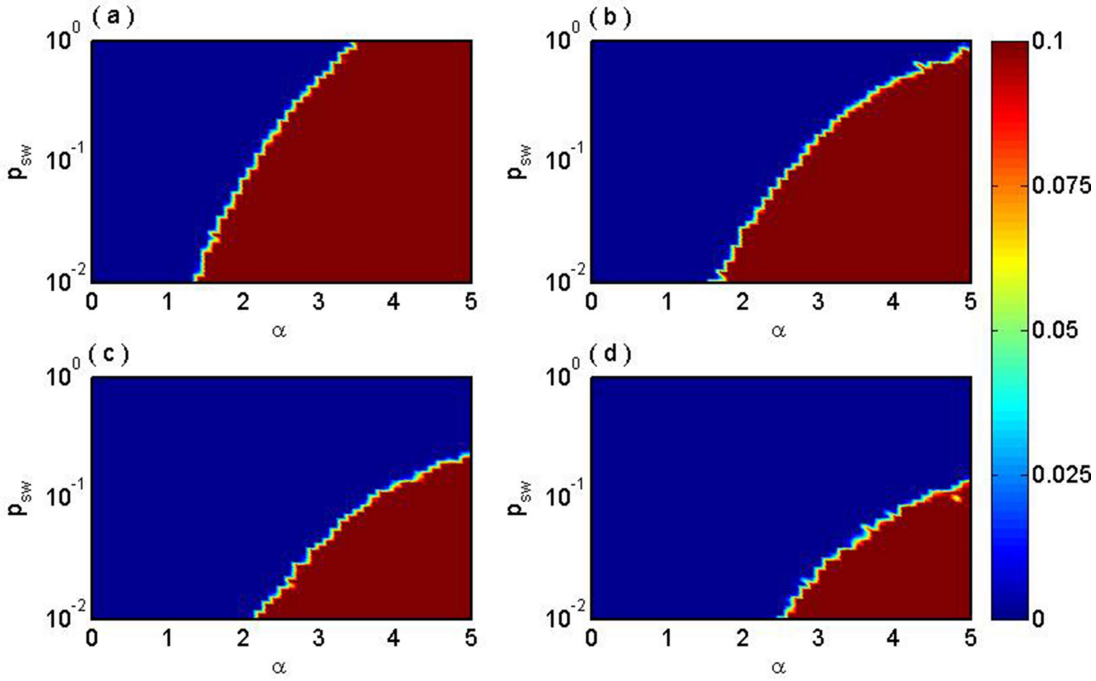


**FIG. 4.** Dependency of complete neuronal synchronization on the gap-junctional strength $\epsilon$ in the $(\alpha, p_{sw})$ parameter plane for (a) $\epsilon = 0.1$, (b) $\epsilon = 0.2$, (c) $\epsilon = 0.6$, and (d) $\epsilon = 1.0$. The continuous variation of $E$ is depicted in the color bar. Other parameter values are fixed at $p_r = 10^{-3}$ and $k = 3$.

assume that the synchronization solutions of both systems (1) and (6) are identical, i.e., $\mathbf{x}_0 = \mathbf{y}_0$.

If $\delta\mathbf{y}_i(t)$ is the perturbation of the $i$th unit of system (6) from the complete synchronization solution, then we have $\mathbf{y}_i = \mathbf{x}_0 + \delta\mathbf{y}_i(t)$. In vectorial form, the error state variable takes the form $\delta\mathbf{y}(t) = [\delta\mathbf{y}_1(t)^{tr}, \delta\mathbf{y}_2(t)^{tr}, \ldots, \delta\mathbf{y}_N(t)^{tr}]^{tr}$. Then the dynamics of this perturbed variable reads as follows:

$$\delta\dot{\mathbf{y}}(t) = \left[I_N \otimes JF(\mathbf{x}_0) - \sum_{k=1}^{K_{max}} \epsilon_k \bar{\mathscr{L}}^{[k]} \otimes \Gamma\right] \delta\mathbf{y}. \tag{7}$$

$\bar{\mathscr{L}}^{[k]}$ is orthogonally diagonalizable by $V^{[k]}$; thus, $V^{[k]^{-1}} \bar{\mathscr{L}}^{[k]} V^{[k]} = D^{[k]}$ is a diagonal matrix.

Then, we perform the Schur transformation $\eta^{(\mathbf{y})} = (V^{[1]} \otimes I_l)^{-1} \delta\mathbf{y}$. The equation of motion of the transformed perturbed variable is

$$\dot{\eta}^{(\mathbf{y})}(t) = \left[I_N \otimes JF(\mathbf{x}_0) - \sum_{k=1}^{K_{max}} \epsilon_k (V^{[1]^{-1}} \bar{\mathscr{L}}^{[k]} V^{[1]}) \otimes \Gamma\right] \eta^{(\mathbf{y})}. \tag{8}$$

$V^{[1]^{-1}} \bar{\mathscr{L}}^{[k]} V^{[1]} = \begin{Bmatrix} 0 & O_{1\times N-1} \\ O_{N-1\times 1} & \bar{U}^{[k]} \end{Bmatrix}$, where $\bar{U}^{[k]} \in \mathbb{R}^{N-1\times N-1}$.

Thus, the transformed variables $\eta^{(\mathbf{y})}(t)$ yield the decomposition $\eta^{(\mathbf{y})} = [\eta_P^{(\mathbf{y})}\ \eta_T^{(\mathbf{y})}]$, where $\eta_P^{(\mathbf{y})} \in \mathbb{R}^d$, $\eta_T^{(\mathbf{y})} \in \mathbb{R}^{(N-1)d}$. Here, $\eta_P^{(\mathbf{y})}$ corresponds to the perturbation parallel to the synchronization manifold, and $\eta_T^{(\mathbf{y})}$ corresponds to the perturbation transverse to the synchronization manifold. Hence, the parallel and transverse component obeys the evolution equation

$$\dot{\eta}_P^{(\mathbf{y})} = JF(\mathbf{x}_0)\eta_P^{(\mathbf{y})}, \tag{9a}$$

$$\dot{\eta}_T^{(\mathbf{y})} = \left[I_{N-1} \otimes JF(\mathbf{x}_0) - \sum_{k=1}^{K_{max}} \epsilon_k \bar{U}^{[k]} \otimes \Gamma\right] \eta_T^{(\mathbf{y})}. \tag{9b}$$

Considering the same Schur transformation on the time-varying system (4) as $\eta^{(\mathbf{x})} = (V^{[1]} \otimes I_l)^{-1} \delta\mathbf{x}$, the equation of motion of this transformed variable can be written as

$$\dot{\eta}^{(\mathbf{x})}(t) = \left[I_N \otimes JF(\mathbf{x}_0) - \sum_{k=1}^{K_{max}} \epsilon_k (V^{[1]^{-1}} \mathscr{L}^{[k]}(t) V^{[1]}) \otimes \Gamma\right] \eta^{(\mathbf{x})}(t). \tag{10}$$

Here, $V^{[1]^{-1}} \mathscr{L}^{[k]}(t) V^{[1]} = \begin{Bmatrix} 0 & O_{1\times N-1} \\ O_{N-1\times 1} & U^{[k]}(t) \end{Bmatrix}$, where $U^{[k]}(t) \in \mathbb{R}^{N-1\times N-1}$, which captures the association of Laplacian eigenvectors of the 1-path short-range network with the $k$-path distant networks.

Similarly, decomposing the projected error component into the parallel and transverse direction, we have $\eta^{(\mathbf{x})} = [\eta_P^{(\mathbf{x})}, \eta_T^{(\mathbf{x})}]$. Then, we get the dynamics of these two components as

$$\dot{\eta}_P^{(\mathbf{x})} = JF(\mathbf{x}_0)\eta_P^{(\mathbf{x})}, \tag{11a}$$

$$\dot{\eta}_T^{(\mathbf{x})} = [I_{N-1} \otimes JF(\mathbf{x}_0) - \sum_{k=1}^{K_{max}} \epsilon_k U^{[k]}(t) \otimes \Gamma]\eta_T^{(\mathbf{x})}. \tag{11b}$$

Now,

$$\begin{aligned}
&\bar{\mathscr{L}}^{[k]} = \frac{1}{T}\int_t^{t+T} \mathscr{L}^{[k]}(\tau)\, d\tau \\
&\Rightarrow V^{[1]^{-1}} \mathscr{L}^{[k]} V^{[1]} = \frac{1}{T}\int_t^{t+T} V^{[1]^{-1}} \mathscr{L}^{[k]} V^{[1]}(\tau)\, d\tau \\
&\Rightarrow \begin{Bmatrix} 0 & O_{1\times N-1} \\ O_{N-1\times 1} & \bar{U}^{[k]} \end{Bmatrix} = \frac{1}{T}\int_t^{t+T} \begin{Bmatrix} 0 & O_{1\times N-1} \\ O_{N-1\times 1} & U^{[k]}(\tau) \end{Bmatrix} d\tau \\
&\Rightarrow \bar{U}^{[k]} = \frac{1}{T}\int_t^{t+T} U^{[k]}(\tau)\, d\tau.
\end{aligned}$$

Therefore, we can conclude that the time-varying system (1) consisting of long-range interactions exhibits stable complete synchronization solution whenever the corresponding time-averaged system (6) yields stable synchronization motion.

For local stability of complete synchronous solution, the transverse error dynamics becomes

$$\dot{\eta}_{T_i}^{(\mathbf{y})} = JF(\mathbf{x}_0)\eta_{T_i}^{(\mathbf{y})} - \sum_{k=1}^{K_{max}} \epsilon_k \sum_{j=1}^{N-1} \bar{U}_{ij}^{[k]} \Gamma \eta_{T_j}^{(\mathbf{y})}. \tag{12}$$

Since $\bar{U}^{[1]} = diag\{\bar{\gamma}_1^{[1]}, \bar{\gamma}_2^{[1]}, \ldots, \bar{\gamma}_N^{[1]}\}$, the coupling term corresponding to the 1-path graph can be decoupled. Hence, the required master stability equation becomes

$$\dot{\eta}_{T_i}^{(\mathbf{y})} = [JF(\mathbf{x}_0) - \epsilon_1 \bar{\gamma}_i^{[1]} \Gamma]\eta_{T_i}^{(\mathbf{y})} - \sum_{k=2}^{K_{max}} \epsilon_k \sum_{j=1}^{N-1} \bar{U}_{ij}^{[k]} \Gamma \eta_{T_j}^{(\mathbf{y})}. \tag{13}$$

If $K_{max} = 2$, then there are two time-averaged $k$-path Laplacians, namely, $\bar{\mathscr{L}}^{[1]}$ and $\bar{\mathscr{L}}^{[2]}$. Without any loss of generality, let us assume that $\bar{\mathscr{L}}^{[1]}$ has the eigenvalue 0 with algebraic multiplicity 1 and $\bar{\gamma}^{[1]}$ with algebraic multiplicity $N-1$. Therefore, we get $\bar{\gamma}_i^{[1]} = \bar{\gamma}^{[1]}$ for all $i = 2, 3, \ldots, N$. For this case, the transverse MSE can be written as

$$\dot{\eta}_{T_i}(t) = JF(\mathbf{x}_0)\eta_{T_i}(t) - \epsilon_1 \bar{\gamma} \Gamma \eta_{T_i}(t) - \epsilon_2 \sum_{j=1}^{N-1} \bar{U}_{ij}^{[2]} \Gamma \eta_{T_j}(t). \tag{14}$$

Note that $\bar{U}^{[2]}$ obeys $V^{[1]^{-1}} \bar{\mathscr{L}}^{[2]} V^{[1]} = \begin{bmatrix} 0 & O_{1\times N-1} \\ O_{N-1\times 1} & \bar{U}^{[2]} \end{bmatrix}$. Moreover, $\bar{\mathscr{L}}^{[2]}$ is symmetric and it is orthogonally diagonalizable by its basis of eigenvector $V^{[1]}$. This implies $V^{[1]^{-1}} = V^{[1]^{tr}}$, and therefore

$$\left(V^{[1]^{-1}} \bar{\mathscr{L}}^{[2]} V^{[1]}\right)^{tr} = V^{[1]^{tr}} \bar{\mathscr{L}}^{[2]} V^{[1]}.$$

So, the matrix $\begin{bmatrix} 0 & O_{1\times N-1} \\ O_{N-1\times 1} & \bar{U}^{[2]} \end{bmatrix}$ is symmetric and hence $\bar{U}^{[2]}$ is also symmetric. Therefore, $\bar{U}^{[2]}$ can be diagonalized orthogonally by the basis of eigenvectors $W$.

Now, with the Schur transformation $\xi(t) = [W \otimes I_l]^{-1} \eta_T(t)$, we get the dynamics of $\xi(t)$ as

$$\begin{aligned}
\dot{\xi}(t) &= [W \otimes I_l]^{-1} \dot{\eta}_T(t) \\
&= \left[I_{N-1} \otimes JF(\mathbf{x}_0) - \epsilon_1 \gamma I_{N-1} \otimes \Gamma - \epsilon_2 W^{-1} \bar{U}^{[2]} W \otimes \Gamma\right] \xi(t).
\end{aligned}$$

As $W^{-1}\bar{U}^{[2]}W = \text{diag}\{\bar{\gamma}_1^{[3]}, \bar{\gamma}_2^{[3]}, \ldots \bar{\gamma}_{N-1}^{[3]}\}$, where $\bar{\gamma}_i^{[3]}$ $(1 \le i \le N-1)$ are the eigenvalues of $\bar{U}^{[2]}$. So, one can get the required MSE as

$$\dot{\xi}_i(t) = \left[JF(\mathbf{x}_0) - \epsilon_1 \bar{\gamma} \Gamma - \epsilon_2 \bar{\gamma}_i^{[3]} \Gamma\right] \xi_i(t), \tag{15}$$

which are $N-1$ number of uncoupled $l$-dimensional systems.

Therefore, we are able to decouple the error dynamics transverse to the synchronization manifold as $N-1$ number of $l$-dimensional dynamical units if the following conditions hold

1. $K_{max} = 2$,
2. for these two time-averaged $k$-path Laplacians, one has eigenvalues 0 and $\bar{\gamma}^{[1]}$ with respective algebraic multiplicities 1 and $N-1$.

Now, for sufficiently rapid switching, the coupled neurons with the rapidly time-varying network and the time-averaged network yield an identical synchronization transition. The time-averaged neuronal system corresponding to the time-varying system (2) can be written as

$$\begin{aligned}
\dot{x}_i &= y_i - a x_i^3 + b x_i^2 - z_i + I + \epsilon \sum_{k=1}^{K_{\max}} \frac{1}{k^\alpha} \sum_{j=1}^{N} \bar{\mathscr{A}}_{ij}^{[k]} (x_j - x_i), \\
\dot{y}_i &= c - d x_i^2 - y_i, \\
\dot{z}_i &= r(s(x_i - x_0) - z_i),
\end{aligned} \tag{16}$$

where $K_{max} = \max\{k_{max}(t) : t \in \mathbb{R}^+\}$.

Next, we examine the stability of the synchronous solution of the time-averaged system (16). Here, all the isolated neuron dynamics are identical and coupled among themselves through mutual diffusive coupling. Moreover, the identical isolated neuron dynamics and the interaction function both are continuously differentiable. Therefore, through the MSF formalism, the stability criterion can be derived, which is necessary and sufficient for infinitesimal perturbations.

When the neuronal synchrony emerges, let each neuron synchronously resides on the manifold $[x(t), y(t), z(t)]$ of synchrony. As a result, we can write the transverse MSE for the ensemble of HR neuronal oscillators as

$$\begin{aligned}
\dot{\xi}_i^{(x)} &= (-3ax^2 + 2bx)\xi_i^{(x)} + \xi_i^{(y)} - \xi_i^{(z)} - \epsilon \sum_{k=2}^{K_{max}} \frac{1}{k^\alpha} \sum_{j=2}^{N} \bar{U}_{ij-1}^{[k]} \xi_j^{(x)}, \\
\dot{\xi}_i^{(y)} &= -2\, dx \xi_i^{(x)} - \xi_i^{(y)}, \\
\dot{\xi}_i^{(z)} &= r(s\xi_i^{(x)} - \xi_i^{(z)}), \quad i = 2, 3, \ldots, N.
\end{aligned} \tag{17}$$

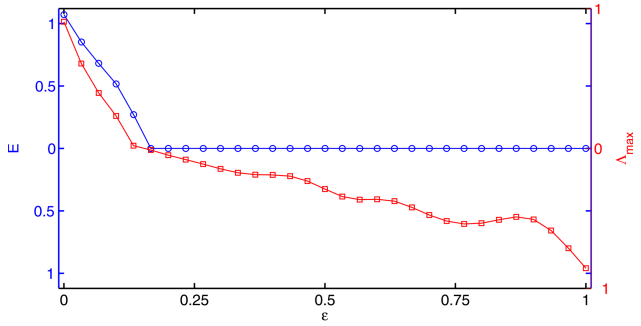


**FIG. 5.** Variation of $E$ (blue circle curve) (for sufficient fast-switching $p_r = 10^0$) and the maximum transverse Lyapunov exponent $\Lambda_{max}$ (red square curve) as functions of the synaptic strength $\epsilon$. Other parameters are $\alpha = 2.5$, $p_{sw} = 0.1$, and $k_{sw} = 3$.

Here, $(x, y, z)$ is the state vector corresponding to the manifold of synchrony, which follows

$$\begin{aligned} \dot{x} &= x^2(b - ax) + y - z + I, \\ \dot{y} &= c - dx^2 - y, \\ \dot{z} &= r(s(x - x_0) - z). \end{aligned} \tag{18}$$

With respect to the parameters $\epsilon$, $\alpha$, $p_{sw}$, and $k$, the maximum Lyapunov exponent $\Lambda_{max}$ of the above master stability equation (17) gives the necessary and sufficient condition for stability of neuronal synchronization. For the local asymptotic stability of the state of synchronization, perturbations should asymptotically vanish along all transverse directions. Therefore, the maximum Lyapunov exponent of Eq. (17) must be negative.

In Fig. 5, we have plotted the variation fo the synchronization error $E$ by changing $\epsilon$ for $p_r = 10^0$, $\alpha = 2.5$, $p_{sw} = 0.1$, and $k_{sw} = 3$. As we have set the values of the rewiring probability to 1, the underlying network is sufficiently fast-switching. Now, the transition from desynchronization to synchronization is quantified through $\Lambda_{max}$. Here, $\Lambda_{max}$ crosses the zero line precisely at the point where $E$ becomes zero. This implies that the analytically derived condition well agrees with numerically obtained synchronization error plot.

## VI. CONCLUSION

In the literature, there are a large number of results relating to the study of synchronization phenomena in networks having diverse complex architectures including static long-range underlying networks or temporal short-range interactions. But, there is a gap in exploring this phenomenon in systems undergoing time-varying long-range interactions. Besides the 1-path Laplacian matrix for direct communications, a long-range interaction essentially deals with each and every other feasible $k$ ($> 1$)-path interactions among every pair of nodes manifested in terms of the $k$ ($> 1$)-path Laplacians.

In this article, complete synchronization in neuronal ensembles is investigated over the small-world network model subject to time-varying long-range interactions. Specifically, we have dealt with a neuronal network comprising direct as well as indirect connections and have explored the emergence of synchrony. The long-range couplings are modeled through coupling strength between the neurons subject to a power-law decay. We have analyzed the Hindmarsh–Rose neuronal model to describe the dynamics of the neurons in the network, with electric gap junctional synaptic communications for direct as well as indirect connections. As mentioned, here we have contemplated with connections beyond static short-range and dealt with time-varying long-range interactions, with a network rewiring probability $p_r$. The synaptic strength needed for complete synchronization is found to be lower when the underlying network rapidly switches. This signifies larger windows of complete neuronal synchrony induced by fast switching networks. Next, adopting the master stability function framework and fast switching stability criteria, we have investigated the local stability of this state. This way, we demonstrated how synchrony appears depending on the network rewiring probability, synaptic strength, and power-law decay rate. Interestingly, a rigorous analysis on the local stability of neuronal synchronization is presented based on the master stability function framework for our considered temporal long-range neuronal network. We hope that our work will strengthen the understanding of emerging neuronal activities in time-varying long-range networks. Hence, our study may trigger future research works on some of the open concerns arising from this article, also future investigation of more realistic models.

## DATA AVAILABILITY

The data that support the findings of this study are available within the article.

## REFERENCES

[1]E. Rybalova, V. S. Anishchenko, G. I. Strelkova, and A. Zakharova, Chaos **29**, 071106 (2019).
[2]E. Rybalova, A. Bukh, G. Strelkova, and V. Anishchenko, Chaos **29**, 101104 (2019).
[3]N. I. Semenova, G. I. Strelkova, V. S. Anishchenko, and A. Zakharova, Chaos **27**, 061102 (2017).
[4]E. V. Rybalova, T. E. Vadivasova, G. I. Strelkova, V. S. Anishchenko, and A. S. Zakharova, Chaos **29**, 033134 (2019).
[5]M. E. J. Newman, *Networks: An Introduction* (Oxford University Press, Oxford, 2010).
[6]R. Albert and A.-L. Barabási, Rev. Mod. Phys. **74**, 47 (2002).
[7]A. Arenas, A. Díaz-Guilera, J. Kurths, Y. Moreno, and C. Zhou, Phys. Rep. **469**, 93 (2008).
[8]A. Pikovsky, M. Rosenblum, and J. Kurths, *Synchronization: A Universal Concept in Nonlinear Science* (Cambridge University Press, 2003).
[9]S. Boccaletti, J. Kurths, G. Osipov, D. L. Valladares, and C. S. Zhou, Phys. Rep. **366**, 1 (2002).
[10]Y. C. Lai and C. Grebogi, Phys. Rev. E **47**, 2357 (1993).
[11]P. Holme and J. Saramäki, Phys. Rep. **519**, 97 (2012).
[12]M. Frasca, A. Buscarino, A. Rizzo, L. Fortuna, and S. Boccaletti, Phys. Rev. Lett. **100**, 044102 (2008).
[13]V. Kohar, P. Ji, A. Choudhary, S. Sinha, and J. Kurths, Phys. Rev. E **90**, 022812 (2014).
[14]S. Rakshit, S. Majhi S, B. K. Bera, S. Sinha, and D. Ghosh, Phys. Rev. E **96**, 062308 (2017).
[15]N. Fujiwara, J. Kurths, and A. Díaz-Guilera, Phys. Rev. E **83**, 025101 (2011).

[16]S. Rakshit, B. K. Bera, E. M. Bollt, and D. Ghosh, SIAM J. Appl. Dyn. Syst. **19**, 918 (2020).
[17]S. Majhi, D. Ghosh, and J. Kurths, Phys. Rev. E **99**, 012308 (2019).
[18]M. Porfiri, D. J. Stilwell, E. M. Bollt, and J. D. Skufca, Physica D **224**, 102 (2006).
[19]S. Rakshit, B. K. Bera, and D. Ghosh, Phys. Rev. E **98**, 032305 (2018).
[20]I. V. Belykh, V. N. Belykh, and M. Hasler, Physica D **195**, 188 (2004).
[21]R. Jeter and I. Belykh, IEEE Trans. Circuits Syst. I **62**, 1260 (2015).
[22]S. Majhi and D. Ghosh, Chaos **27**, 053115 (2017).
[23]A. Mondal, S. Sinha, and J. Kurths, Phys. Rev. E **78**, 066209 (2008).
[24]S. Boccaletti, D. -U. Hwang, M. Chavez, A. Amann, J. Kurths, and L. M. Pecora, Phys. Rev. E **74**, 016102 (2006).
[25]A. Campa, T. Dauxois, and S. Ruffo, Phys. Rep. **480**, 57 (2009).
[26]S. Gupta and D. Mukamel, Phys. Rev. Lett. **105**, 040602 (2010).
[27]A. Campa, T. Dauxois, D. Fanelli, and S. Ruffo, *Physics of Long-Range Interacting Systems* (Oxford University Press, Oxford, 2014).
[28]S. Gupta and S. Ruffo, Int. J. Mod. Phys. **A32**, 1741018 (2017).
[29]S. A. Cannas and F. A. Tamarit, Phys. Rev. B **54**, R12661 (1996).
[30]G. Kotliar, P. W. Anderson, and D. L. Stein, Phys. Rev. B **27**, 602 (1983).
[31]B. G. Szaro and R. Tompkins, J. Comput. Neurol. **258**, 304 (1987).
[32]Y. Levin, R. Pakter, and T. N. Teles, Phys. Rev. Lett. **100**, 040604 (2008).
[33]D. E. Bowler and T. G. Benton, Oikos **118**, 403 (2009).
[34]Z. Frica and M. Konvicka, Basic Appl. Ecol. **8**, 377 (2007).
[35]C. Anteneodo, A. M. B. S. E. S. Pinto, and R. L. Viana, Phys. Rev. E **68**, 045202(R) (2003).
[36]H.-Y. Kuo and K.-A. Wu, Phys. Rev. E **92**, 062918 (2015).
[37]S. Raghavachari and J. A. Glazier, Phys. Rev. Lett. **74**, 3297 (1995).
[38]J. L. Rogers and L. T. Wille, Phys. Rev. E **54**, R2193 (1996).
[39]M. Maródi, F. d'Ovidio, and T. Vicsek, Phys. Rev. E **66**, 011109 (2002).
[40]D. Chowdhury and M. C. Cross, Phys. Rev. E **82**, 016205 (2010).
[41]C. Anteneodo, S. E. S. Pinto, A. M. Batista, and R. L. Viana, Phys. Rev. E **68**, 045202(R) (2003).
[42]E. Estrada, L. V. Gambuzza, and M. Frasca, SIAM J. Appl. Dyn. Syst. **17**, 672 (2018).
[43]K. Sathiyadevi, V. K. Chandrasekar, D. V. Senthilkumar, and M. Lakshmanan, J. Phys. A: Math. Theor. **52**, 184001 (2019).
[44]A. Gupta, T. Banerjee, and P. S. Dutta, Phys. Rev. E **96**, 042202 (2017).
[45]C. I. Del Genio, J. Gómez-Gardeñes, I. Bonamassa, and S. Boccaletti, Sci. Adv. **2**, e1601679 (2016).
[46]S. Wasserman and K. Faust, *Social Network Analysis: Methods and Applications* (Cambridge University Press, Cambridge, 1994).
[47]R. Pastor-Satorras and A. Vespignani, *Evolution and Structure of the Internet: A Statistical Physics Approach* (Cambridge University Press, Cambridge, 2004).
[48]R. Olfati-Saber, J. A. Fax, and R. M. Murray, Proc. IEEE **95**, 215 (2007).
[49]M. Frasca, A. Buscarino, A. Rizzo, L. Fortuna, and S. Boccaletti, Phys. Rev. E **74**, 036110 (2006).
[50]M. Valencia, J. Martinerie, S. Dupont, and M. Chavez, Phys. Rev. E **77**, 050905(R) (2008).
[51]J.-P. Onnela, J. Saramaki, J. Hyvonen, G. Szabo, D. Lazer, K. Kaski, J. Kertesz, and A. L. Barabasi, Proc. Natl. Acad. Sci. U.S.A. **104**, 7332 (2007).
[52]M. L. Sachtjen, B. A. Carreras, and V. E. Lynch, Phys. Rev. E **61**, 4877 (2000).
[53]D. Tanaka, Phys. Rev. Lett. **99**, 134103 (2007).
[54]F. Sivrikaya and B. Yener, IEEE Netw. **18**, 45 (2004).
[55]S. Lèbre, J. Becq, F. Devaux, M. P. H. Stumpf, and G. Lelandais, BMC Syst. Biol. **4**, 130 (2010); A. Rao, A. O. Hero, D. J. States, and J. D. Engel, EURASIP J. Bioinf. Syst. Biol. **2007**, 51947..
[56]M. Uzuntarla, Neurocomputing **367**, 328–336 (2019).
[57]M. Uzuntarla, E. Barreto, and J. J. Torres, PLoS Comput. Biol. **13**, e1005646 (2017).
[58]Z. Wang, S. Baruni, F. Parastesh, S. Jafari, D. Ghosh, M. Perc, and I. Hussain, Neurocomputing **406**, 117–126 (2020).
[59]D. S. Bassett, N. F. Wymbs, M. A. Porter, P. J. Mucha, J. M. Carlson, and S. T. Grafton, Proc. Natl. Acad. Sci. U.S.A. **108**, 7641 (2011).
[60]D. Guo, Q. Wang, and M. Perc, Phys. Rev. E **85**, 061905 (2012).
[61]S. N. Agaoglu, A. Calim, P. Hövel, M. Ozer, and M. Uzuntarla, Neurocomputing **325**, 59–66 (2019).
[62]K. Pal, D. Ghosh, and G. Gangopadhyay, Neurocomputing **422**, 222–234 (2021).
[63]H. Fan, Y. Wang, H. Wang, Y. C. Lai, and X. Wang, Sci. Rep. **8**, 580 (2018).
[64]M. S. Santos, P. R. Protachevicz, K. C. Iarosz, I. L. Caldas, R. L. Viana, F. S. Borges, H. P. Ren, J. D. Szezech, Jr., A. M. Batista, and C. Grebogi, Chaos **29**, 043106 (2019).
[65]D. S. Bassett and E. T. Bullmore, Neuroscientist **23**, 499 (2017).
[66]C. C. Hilgetag and A. Goulas, Brain Struct. Funct. **221**, 2361 (2016).
[67]T. R. Knösche and M. Tittgemeyer, Front. Syst. Neurosci. **5**, 58 (2011).
[68]A. T. L. Leong, R. W. Chan, P. P. Gao, Y.-S. Chan, K. K. Tsia, W.-H. Yung, and E. X. Wu, Proc. Natl. Acad. Sci. U.S.A. **113**, E8306 (2016).
[69]F. Wolf, Phys. Rev. Lett. **95**, 208701 (2005).
[70]P. Wang, F. Göschl, U. Friese, P. König, and A. K. Engel, NeuroImage **196**, 114 (2019).
[71]D. J. Watts and S. H. Strogatz, Nature **393**, 440 (1998).
[72]E. R. Kandel, J. H. Schwartz, and T. M. Jessell, *Principles of Neural Science* (McGraw-Hill, New York, 2000), ISBN 0-8385-7701-6.
[73]Q. Chang, A. Pereda, M. J. Pinter, and R. J. Balice-Gordon, J. Neurosci. **20**, 674 (2000).
[74]M. V. Bennett and R. S. Zukin, Neuron **41**, 495 (2004).
[75]M. S. Baptista, F. M. Moukam Kakmeni, and C. Grebogi, Phys. Rev. E **82**, 036203 (2010).
[76]D. S. Bassett and E. Bullmore, Neuroscientist **12**, 512 (2006).
[77]X. Liao, A. V. Vasilakos, and Y. He, Neurosci. Biobehav. Rev. **77**, 286 (2017).
[78]D. S. Bassett, A. Meyer-Lindenberg, S. Achard, T. Duke, and E. Bullmore, Proc. Natl. Acad. Sci. U.S.A. **103**, 19518 (2006).
[79]S. F. Muldoon, E. W. Bridgeford, and D. S. Bassett, Sci. Rep. **6**, 22057 (2016).
[80]D. J. Stilwell, E. M. Bollt, and D. G. Roberson, SIAM J. Appl. Dyn. Syst. **5**, 140 (2006).
[81]L. M. Pecora and T. L. Carroll, Phys. Rev. Lett. **80**, 2109 (1998).